Int J Clin Exp Med 2015;8(9):15362-15372
www.ijcem.com /ISSN:1940-5901/IJCEM0012834

Original Article

The diagnosis value of acoustic radiation force impulse (ARFI) elastography for thyroid malignancy without highly suspicious features on conventional ultrasound

Bo-Ji Liu[1,2*], Feng Lu[1,2*], Hui-Xiong Xu[1,2,3], Le-Hang Guo[1,2], Dan-Dan Li[1,2], Xiao-Wan Bo[1,2], Xiao-Long Li[1,2], Yi-Feng Zhang[1,2], Jun-Mei Xu[1,2], Xiao-Hong Xu[3], Shen Qu[2,4]

[1]Department of Medical Ultrasound, Shanghai Tenth People's Hospital, Ultrasound Research and Education Institute, Tongji University School of Medicine, Shanghai 200072, China; [2]Thyroid Institute, Tongji University School of Medicine, Shanghai 200072, China; [3]Department of Ultrasound, Guangdong Medical College Affiliated Hospital, Zhanjiang 524001, China; [4]Department of Endocrinology and Metabolism, Shanghai Tenth People's Hospital, Tongji University School of Medicine, Shanghai 200072, China. [*]Equal contributors.

Received July 13, 2015; Accepted September 1, 2015; Epub September 15, 2015; Published September 30, 2015

Abstract: Objective: The aim of this study was to evaluate the potential diagnostic performance of acoustic radiation force impulse (ARFI) elastography in identifying malignancy in nodules that do not appear highly suspicious on conventional ultrasound (US). Methods: 330 pathologically confirmed thyroid nodules (40 malignant and 290 benign; mean size, 22.0±11.6 mm) not suspicious of malignancy on conventional US in 330 patients (mean age 52.8±11.7 years) underwent ARFI elastography before surgery. ARFI elastography included qualitative ARFI-induced strain elastography (SE) and quantitative point shear wave elastography (p-SWE). ARFI-induced SE image was assessed by SE score, while p-SWE was denoted with shear wave velocity (SWV, m/s). The diagnostic performance of four criteria sets was evaluated: criteria set 1 (ARFI-induced SE), criteria set 2 (p-SWE), criteria set 3 (either set 1 or 2), criteria set 4 (both set 1 and 2). Receiver operating characteristic curve (ROC) analyses were performed to assess the diagnostic performance. Results: SE score ≥4 was more frequently found in malignant nodules (32/40) than in benign nodules (30/290, P<0.001). The mean SWV of malignant nodules (3.64±2.23 m/s) was significantly higher than that of benign nodules (2.02±0.69 m/s) (P<0.001). ARFI-induced SE (set 1) had a sensitivity of 80.0% (32/40) and a specificity of 89.7% (260/290) with a cut-off point of SE score ≥4; p-SWE (set 2) had a sensitivity of 80.0% (32/40) and a specificity of 57.9% (168/290) with a cut-off point of SWV ≥2.15 m/s. When ARFI-induced SE and p-SWE were combined, set 3 had the highest sensitivity (92.5%, 37/40) while set 4 had the highest specificity (95.2%, 276/290). Conclusion: ARFI elastography can be used for differential diagnosis of malignant thyroid nodules without highly suspicious features on US. The combination of ARFI-induced SE and p-SWE leads to improved sensitivity and specificity.

Keywords: Ultrasound, thyroid, elastography, acoustic radiation force impulse, thyroid malignancy

Introduction

According to the recommendations of American Thyroid Association (ATA) guideline about thyroid nodules, thyroid ultrasound (US) examination should be performed in all patients with thyroid nodules [1]. Approximately 68% of the general population have thyroid nodules by high-resolution US and 5%-15% of them are malignant [2]. The differential diagnosis between benign and malignant thyroid nodules on US depends on the prevalence of suspicious characteristics including solid component, hypoechogenicity or marked hypoechogenicity, microcalcification, taller-than-wide shape and microlobulated or irregular margin [3-5]. However, up to 55% of benign nodules are also hypoechoic compared with thyroid parenchyma, making the feature of nodule hypoechogenicity less specific [4]. In addition, papillary thyroid carcinomas (PTCs) without highly suspicious features on conventional US account for approximately 15% of all PTCs [6]. Some malignant nodules may be misdiagnosed due to the absence of typical suspicious features on US. Therefore, the sensitivity of conventional US in

diagnosing malignant thyroid nodules varies from 38.8% to 90.9% [7-10], which causes a dilemma in management of those thyroid malignancies without highly suspicious features on US.

Fine needle aspiration cytology (FNAC) is the most accurate method for diagnosis of thyroid nodule and for selection of nodules for surgery, with a sensitivity range of 83%-100% and a specificity range of 60%-96% [11-13]. FNAC is recommended for solid thyroid nodule more than 1 cm in diameter according to ATA guidelines [1]. However, since it is an invasive and somewhat expensive procedure, many patients are reluctant to undergo FNAC. In addition, 3% to 22% FNAC results are non-diagnostic, so approximately 10%-30% of patients undergo diagnostic thyroid lobectomy for a benign diagnosis [14-16]. Finally, in consideration of a large amount of thyroid nodules detected in daily clinical practice, it is impossible to perform FNAC for all of them. Acoustic radiation force impulse (ARFI) elastography is a new technique used in parenchymal organs in recent years [17-20]. It is a novel US-based elastography method enabling qualitative and quantitative evaluation of tissue stiffness. Transverse shear wave propagation is generated when the target tissue within the sampling box is excited by an acoustic push pulse transmitted from the transducer. The strain change caused by the push pulse is named as virtual touch tissue imaging (VTI) (Siemens Medical Solutions, Mountain View, Calif, USA), which is a type of ARFI-induced strain elastography (SE) and is displayed as a grayscale image; while quantitative evaluation of the tissue stiffness is virtual touch tissue quantification (VTQ) (Siemens Medical Solutions, Mountain View, Calif, USA), which is point shear wave elastography (p-SWE). The diagnostic value of ARFI elastography for thyroid nodules in general population has been confirmed by several studies that showed a sensitivity range of 74.2%-87.0% for ARFI-induced SE and a sensitivity range of 57.0-90.9% for p-SWE [21-26]. However, to the best of our knowledge, no reports have been published to explore the diagnostic performance of ARFI elastography for thyroid nodules without highly suspicious features on US.

The aims of this study were to retrospectively evaluate the potential diagnostic performance of ARFI elastography in identifying malignancy in nodules that do not appear highly suspicious on conventional US and to explore the potential improvement in this performance by combining ARFI-induced SE with p-SWE.

Methods and materials

Patients

This retrospective study was approved by the Ethical Committee of the university hospital and informed consent was waived. Patients were included if they met the following inclusion criteria: (A) nodules with diameter ≥5 mm showed on conventional US; (B) the patients received conventional US and ARFI elastography examinations before surgery; (C) pathological confirmation was obtained after the examinations. Patients were excluded when (A) one or more accepted typical suspicious features showed on conventional US; (B) cystic portion was more than 50%; (C) the nodule area without cyst and calcification was smaller than the 6x5 mm sampling region of interest (ROI); (D) complete data were not available on US and ARFI elastography. The accepted highly suspicious US features included marked hypoechogenicity (echogenicity lower than that of the surrounding strap muscle), infiltrative border, taller-than-wide shape (greater in the anteroposterior dimension than the transverse dimension) and intranodular microcalcifications (calcifications equal to or less than 1 mm in diameter and visualized as tiny punctate hyperechoic foci) [3, 6, 7, 27]. The nodules included in this study were nodules without any of the abovementioned accepted highly suspicious US features.

One thyroid nodule was selected for analysis per patient. If nodules with and without highly suspicious features were coexisting, nodule without highly suspicious features was selected; When multiple nodules that were not highly suspicious of malignancy existed, the largest one was selected for evaluation. The flowchart of nodule selection was presented in **Figure 1**. Finally, 330 nodules (mean size, 22.0±11.6 mm; range, 5-62 mm) from 330 patients (80 men and 250 women; mean age, 52.8±11.7 years old; range, 21-78 years old) were included from April 2011 to September 2013. All of the nodules in this study underwent surgery. The indications for thyroidectomy were as follows: (1) confirmed or suspicious of malignancy by

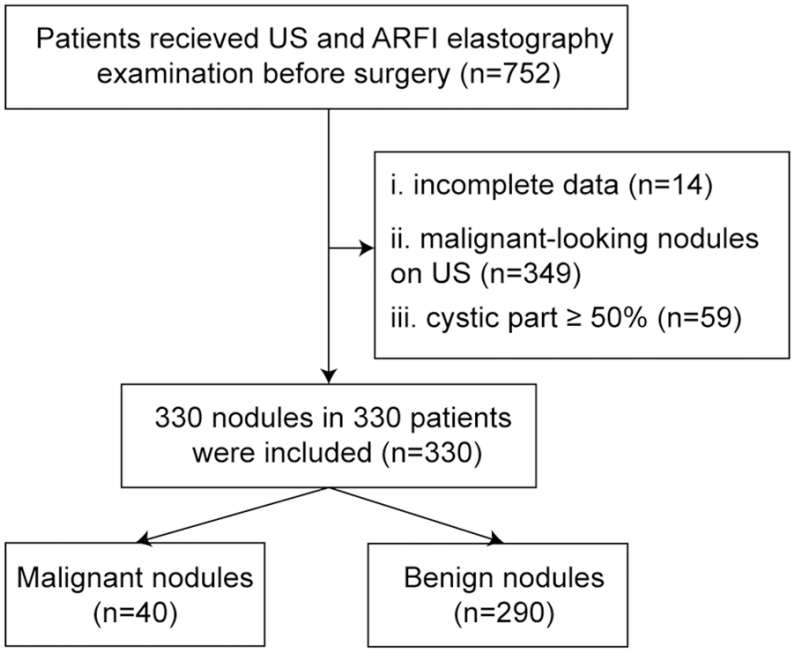

Figure 1. The diagram of nodule selection for the included patients. Malignant-looking nodule was defined as nodule without marked hypoechogenicity, infiltrative border, taller-than-wide shape or microcalcification on ultrasound image. US, ultrasound; ARFI, acoustic radiation force impulse; n, number of patients.

FNAC; (2) non-diagnostic, indeterminate results or follicular lesions detected by FNAC; (3) patients' anxiety and refusal of FNAC; (4) compressive symptoms caused by large nodules or associated large nodules.

Conventional ultrasound (US) examination

Conventional US and ARFI elastography were performed using the same S2000 US scanner (Siemens Medical Solutions, Mountain View, Calif, USA) containing a 4-9 MHz linear transducer by one of two investigators with ten years of experience in US and three years of experience in US elastography. The patients were lying in the supine position with dorsal flexion of the head to make the neck skin fully exposed. The coupling medium was smeared on the US transducer to reduce interference of air with skin and probe. For each thyroid nodule, the maximal diameter was measured and US images were recorded.

ARFI elastography

ARFI elastography was then performed by the same investigator after conventional US as described in the previous literatures [9, 10, 21]. A sampling box was placed on the target nodule while performing real-time B-mode US imaging with some surrounding thyroid tissue. To avoid the influence of pre-compression on the elastic properties of the tissue, the investigator was asked to place the transducer gently on the skin surface with minimum pressure. The patient was required to hold the breath and the transducer was motionless during the acquisition of the elastic images [28]. Tissue within the sampling box was mechanically excited using acoustic pulses to generate localized tissue displacements, which resulted in ARFI-induced SE [21]. ARFI-induced SE which qualitatively evaluated the tissue stiffness was displayed as a gray scale image and was assessed by SE score. Afterwards, quantitative measurement of p-SWE was started and a region of interest (ROI) was placed on the target nodule with the cystic or calcified areas avoided. The placement of p-SWE ROI was guided by the ARFI-induced SE image. Generally, the ROI was placed at the center of small nodules. As for relatively large nodules, ROI was placed at the solid part, usually the inner peripheral portion of the nodule, with an aim to avoid potential liquefaction or necrosis in the central region. When the nodule was heterogeneous, the ROI was placed at the stiffest location indicated by the ARFI-induced SE image and repeated measurement was then carried out. The quantitative measurement was performed by calculating the shear wave velocity (SWV, m/s). In p-SWE, SWVs of the nodule were measured at least 7 times. The ARFI elastography images were recorded. The whole process of US and ARFI elastography examination lasted approximately 10 minutes.

Image interpretation

Two investigators who were blind to the pathological results independently reviewed the

Table 1. Clinical and conventional US characteristics of the patients with thyroid nodules

Characteristics	Overall	Benign	Malignant	*P*-value
Number of patients	330	290 (87.9%)	40 (12.1%)	NA
Number of nodules	330	290 (87.9%)	40 (12.1%)	NA
Gender (men/women)	80/250	75/215	5/35	0.076
Mean age (years)	52.8±11.7	52.8±12.0	51.5±11.8	0.504
Range	21-78	21-77	23-78	
Nodule size (mm)	22.0±11.6	22.8±11.5	16.2±11.5	0.001*
Range	5-62	6-62	5-52	
Nodule distribution (single/multiple)	94/236	81/209	13/27	0.577
Background of Hashimoto's thyroiditis	59	44 (15.2%)	15 (37.5%)	0.002*
Ultrasound features				
Internal component				0.034*
Complete solid	301	261 (90.0%)	40 (100%)	
Predominantly solid	29	29 (10.0%)	0 (0%)	
Echogenicity				<0.001*
Hyperechoic	4	4 (1.4%)	0 (0%)	
Isoechoic	92	91 (31.4%)	1 (2.5)	
Hypoechoic	114	80 (27.6)	34 (85.0%)	
Mixed echoic	120	115 (39.7%)	5 (12.5%)	
Halo sign (present/absent)	208/122	200/90	8/32	<0.001*

Note: *indicates statistically significant difference. NA, not applicable.

Table 2. ARFI elastography features of benign and malignant thyroid nodules without highly suspicious features on US

Parameters	Benign nodules (n=290)	Malignant nodules (n=40)	*P*-value
SE score			<0.001*
Score 1	1 (0.3%)	0 (0%)	
Score 2	65 (22.4%)	1 (2.5%)	
Score 3	194 (66.9%)	7 (17.5%)	
Score 4	29 (10.0%)	22 (55.0%)	
Score 5	1 (0.3%)	10 (25.0%)	
Score 6	0 (0%)	0 (0%)	
p-SWE			<0.001*
Mean SWV (m/s)	2.02±0.69	3.64±2.23	
Range	0.50-4.40	1.12-8.40	

Note-ARFI, acoustic radiation force impulse; SE, strain elastography; p-SWE, point shear wave elastography; SWV, shear wave velocity. *indicates statistically significant difference.

images and recorded the image interpretations. A third senior investigator reviewed the images and made the final decision in case of discordance in the evaluation between the two investigators. For US images, the following features of nodules were evaluated: nodule size (mm), nodule number (single or multiple), internal component (solid or predominantly solid with partly cystic), echogenicity (hyper-, iso-, hypo-, mixed-) and halo sign (absent or present).

The gray scales of ARFI-induced SE image were classified into 2 categories (white and black) through the comparison between the nodule and the surrounding thyroid tissue. ARFI-induced SE score was categorized according to Xu's VTI scoring system [10, 24] as follows: SE score-1, nearly all white; SE score-2, predominantly white with a few black portions; SE score-3, equal white and black portions; SE score-4, predominantly black with a few white portions; SE score-5, almost completely black; and SE score-6, completely black. Higher SE scores indicated stiffer tissue and higher risk of malignancy. For p-SWE, SWV results were expressed in m/s (range, 0.5-8.4 m/s). The maximal and the minimal SWVs were eliminated and the mean SWV of the nodule were calculated by the remaining 5 measurements. SWVs displayed as "x. xx m/s" were regarded as invalid measurements.

Statistical analysis

To explore the diagnostic performance in differentiating thyroid malignant nodules without

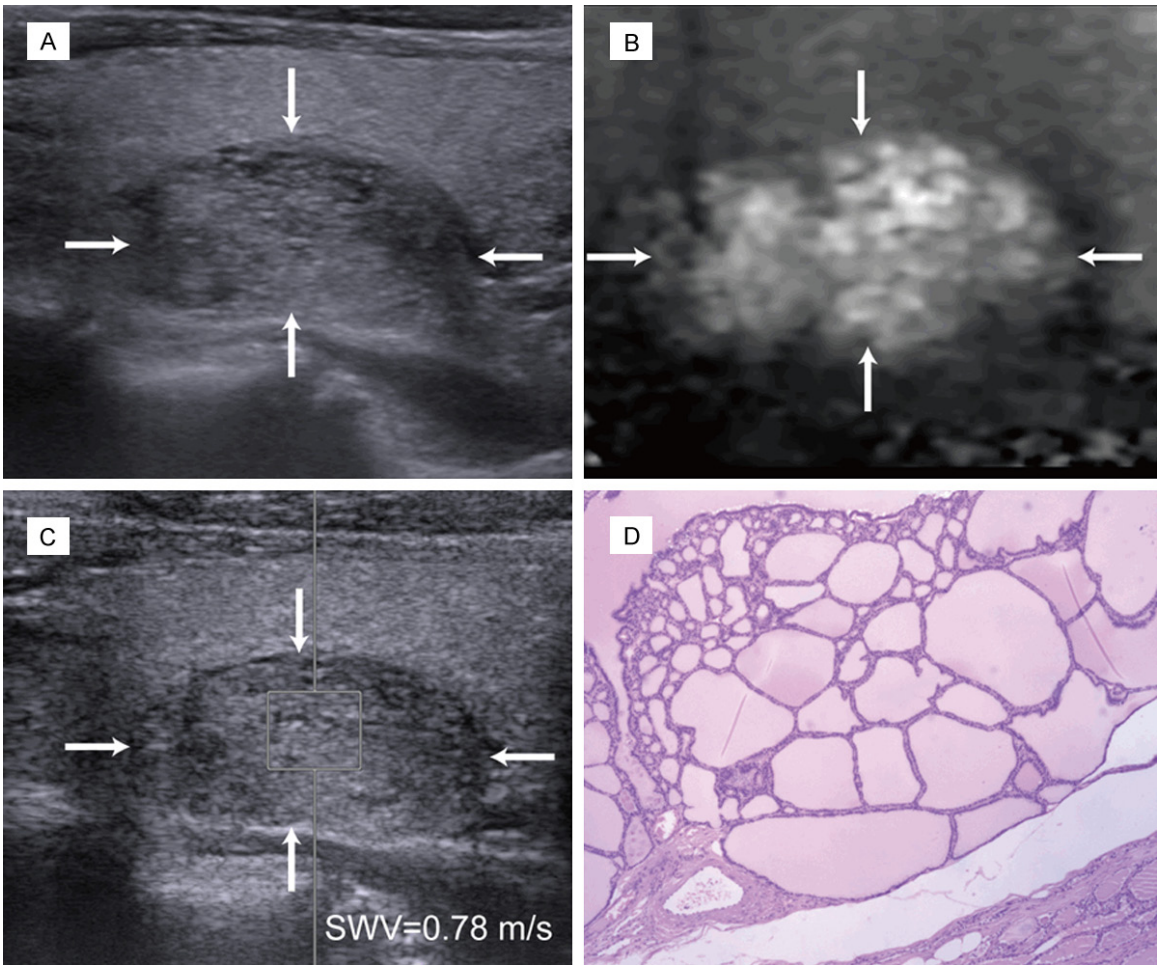

Figure 2. Images in a 56-year-old woman with nodular goiter without highly suspicious features on US. At conventional ultrasound, a 24 mm nodule in the left lobe of the thyroid is solid, mixed-echoic, absence of halo sign (arrows) (A). At ARFI elastography, SE score-1 (arrows) (B), and SWV of 0.78 m/s at p-SWE are assigned (C). The nodule is confirmed to be nodular goiter pathologically (D) (H&E staining, magnification, 10×5). SE, strain elastography; p-SWE, point shear wave elastography; SWV, shear wave velocity.

highly suspicious features on US from benign nodules, the following four sets of criteria were specified: criteria set 1, ARFI-induced SE alone (SE score ≥4); criteria set 2, p-SWE alone (SWV ≥ cut-off point); criteria set 3, either ARFI-induced SE or p-SWE (in compliance with either criteria set 1 or 2); criteria set 4, combination of ARFI-induced SE and p-SWE (in compliance with both criteria set 1 and 2).

Continuous variables were expressed as mean ± standard deviation (SD) and range. Two sets of measurement data and enumeration data were compared by *t* test or χ^2 test, while categorical data by using Mann-Whitney rank sum test of non-parametric tests. The sensitivities, specificities, positive predictive values (PPVs), negative predictive values (NPVs) and accuracies of four criteria sets were calculated. Differences in sensitivity, specificity and accuracy were compared using the Mc Nemar test, while PPV and NPV using χ^2 test. The diagnostic performance of the criteria sets were evaluated by receiver operating characteristic curve (ROC) analysis which was expressed as the area under ROC (AUC) and its 95% confidence interval (CI). Comparison of AUCs was performed by using the method described by Hanley [29]. The cut-off point was obtained when Youden index (sensitivity + specificity-1) reached the maximum value. Odds ratio (OR) value and 95% CI were used to evaluate the association of four criteria sets with malignancy. A two-tailed *P*-value <0.05 indicated statistically significant

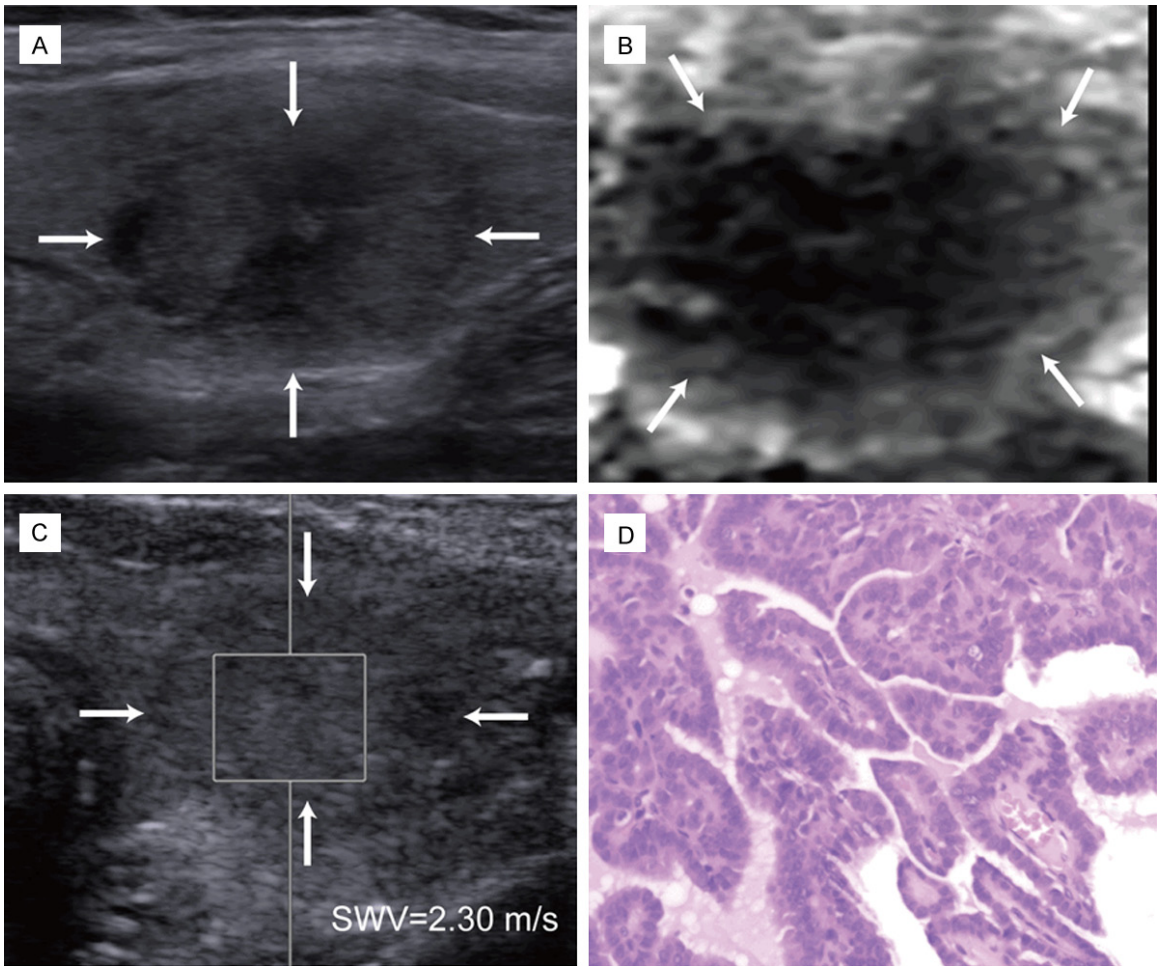

Figure 3. Images in a 45-year-old woman with papillary thyroid carcinoma without highly suspicious features on US. At conventional ultrasound, a 13 mm nodule in the left lobe of the thyroid is solid, isoechoic and hypoechoic, absence of halo sign (arrows) (A). At ARFI elastography, SE score-5 (arrows) (B), and SWV of 2.30 m/s at p-SWE are assigned (C). The nodule is confirmed to be papillary thyroid carcinoma pathologically (D) (H&E staining, magnification, 10×20). SE, strain elastography; p-SWE, point shear wave elastography; SWV, shear wave velocity.

difference. Statistical analysis was performed using SPSS software (version 14.0, Chicago, IL, USA).

Results

Pathological results

All the nodules were confirmed by pathological results after surgery. Of the 330 nodules, 40 were malignant and the remaining 290 were benign. Among the 40 malignant nodules, there were 36 PTCs (90.0%), 2 follicular carcinomas (5.0%), 1 medullary carcinoma (2.5%) and 1 diffuse large B-cell lymphoma (2.5%). The 290 benign nodules included 235 nodular goiters (81.0%), 35 adenomas (12.1%) and 20 Hashimoto's nodules (6.9%).

Conventional US and ARFI elastography features

The differences in conventional US features between malignant and benign nodules without highly suspicious features on US were presented in **Table 1**. Statistically significant differences were found between the two groups in background of Hashimoto's thyroiditis, internal component (P=0.034), echogenicity (P<0.001) and halo sign (P<0.001). Background of Hashimoto's thyroiditis, complete solid component, hypoechogenicity and presence of halo sign were more frequently found in malignant nodules.

The ARFI elastography characteristics were presented in **Table 2**. In ARFI-induced SE, no

Table 3. The diagnostic performance of ARFI elastography for 4 criteria sets

Parameters	Set 1 (ARFI-induced SE)	Set 2 (P-SWE)	Set 3 (ARFI-induced SE or p-SWE)	Set 4 (ARFI-induced SE + P-SWE)
Cut-off point	SE score-4	2.15 m/s	score-4 or 2.15 m/s	score-4 and 2.15 m/s
Sensitivity (%)	80.0 (32/40)	80.0 (32/40)	92.5 (37/40)	67.5 (27/40)
Specificity (%)	89.7* (260/290)	57.9 (168/290)	52.4 (152/290)	95.2#,^ (276/290)
Positive predictive value (%)	51.6* (32/62)	20.8 (32/154)	21.1 (37/175)	65.9 (27/41)
Negative predictive value (%)	97.0 (260/268)	95.5 (168/176)	98.1 (152/155)	95.5 (276/289)
Accuracy (%)	88.5* (292/330)	60.6 (200/330)	57.3 (189/330)	91.8Δ (303/330)
Area under ROC	0.87	0.78	0.73	0.81
95% confidence interval	0.80-0.94	0.70-0.87	0.66-0.80	0.72-0.90
Odds ratio	34.7	5.5	13.6	40.9
95% confidence interval	14.6-82.1	2.5-12.4	4.1-45.1	17.5-96.0

Note-ARFI, acoustic radiation force impulse; SE, strain elastography; SWE, shear wave elastography; ROC, receiver operating characteristic curve. 4 criteria sets: Criteria set 1, SE score ≥4; Criteria set 2, SWV value ≥2.15 m/s; Criteria set 3, in compliance with either criteria set 1 or criteria set 2; Criteria set 4, in compliance with both criteria set 1 and criteria set 2. *P<0.001, in comparison with those in set 2. #P=0.018, in comparison with that in set 1. ^P<0.001, in comparison with that in set 2. ΔP<0.001, in comparison with those in set 2 and set 3.

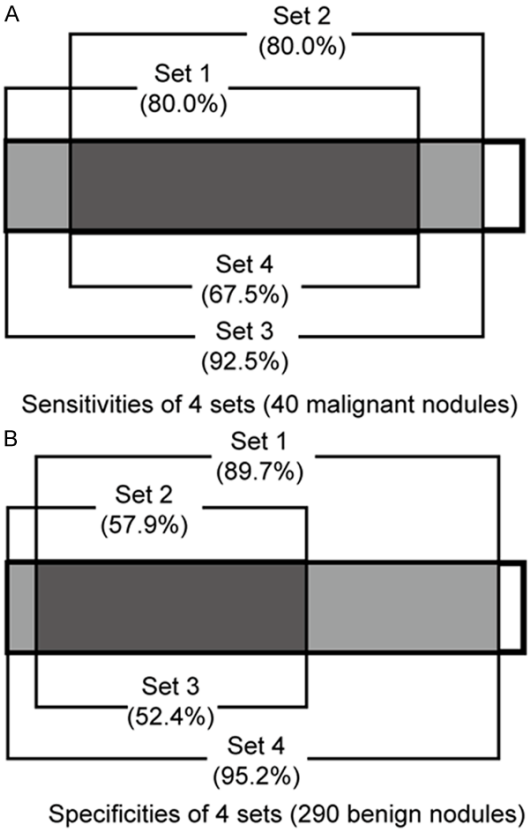

Figure 4. The sensitivities and specificities of four criteria sets. Criteria set 1, ARFI-induced SE (SE score ≥4); set 2, p-SWE (SWV value ≥2.15 m/s); Criteria set 3, in compliance with either criteria set 1 or criteria set 2; Criteria set 4, in compliance with both criteria set 1 and criteria set 2. SE, strain elastography; SWE, shear wave elastography.

nodules were classified as score-6, 11 (3.3%) as score-5, 51 (15.5%) as score-4, 201 (60.9%) as score-3, 66 (20.0%) as score-2, 1 (0.3%) as score-1. Of 330 nodules in ARFI-induced SE, 62 nodules (30 benign and 32 malignant) were classified as SE score ≥4 and the remaining 268 nodules (260 benign and 8 malignant) as SE score ≤3 (P<0.001) (**Figures 2**, **3**). For p-SWE, the mean SWV of malignant nodules (3.64±2.23 m/s) was statistically higher than that of benign nodules (2.02±0.69 m/s) (P<0.001) (**Figures 2**, **3**). The mean SWVs of nodular goiters (n=235, 2.08±0.68 m/s; range, 0.50-4.40 m/s) and Hashimoto's nodules (n=20, 2.15±0.49 m/s; range, 0.81-3.42 m/s) were similar (P=0.628); and they were statistically higher than that of adenomas (n=35, 1.65±0.62 m/s; range, 0.60-3.23 m/s) (both P<0.05) and lower than that of malignant nodules (both P<0.001).

The diagnostic performance of 4 criteria sets

The sensitivities, specificities, PPVs, NPVs, accuracies, AUCs and their 95% CI, ORs and their 95% CI of four criteria sets were shown in **Table 3** and **Figure 4**. The sensitivity and NPV of set 1 was similar to set 2 (both P>0.05), while the specificity, PPV and accuracy of set 1 were statistically higher than that of set 2 (all P<0.01). The sensitivity was improved by set 3 compared with that of set 1 (92.5% vs. 80.0%, P=0.193) and set 2 (92.5% vs. 80.0%, P=0.193). The specificity of set 4 (95.2%) was statistically higher than that of set 1 (95.2% vs. 89.7%, P=0.018) and set 2 (95.2% vs. 57.9%, P<0.001). Of all criteria sets, the criteria set 4 had the highest accuracy (91.8%) compared with set 1 (88.5%, P=0.191), set 2 (60.6%,

P<0.001) and set 3 (P<0.001). No significant differences were found among the criteria sets 1, 2 and 4 in terms of AUCs (all P>0.05), and AUC of criteria set 3 (0.725) was statistically lower than that of criteria set 1 (0.871, P=0.003).

The mean size of false positive (FP) nodules was significantly larger than that of true positive (TP) ones for both ARFI-induced SE (20.5±9.8 mm vs. 13.2±6.4 mm, P=0.001) and p-SWE (21.1±10.9 mm vs. 15.3±10.9 mm, P=0.009). The FP nodules for criteria set 1 (ARFI-induced SE) and set 2 (p-SWE) were 30 (including 26 nodular goiters and 4 Hashimoto's nodules) and 122 (including 107 nodular goiters, 9 Hashimoto's nodules and 6 adenomas) respectively; 16 (53.3%) and 108 (88.5%) of them were correctly diagnosed by criteria set 4. The false negative (FN) nodules for criteria set 1 and set 2 were 8 (6 PTCs, 1 follicular carcinoma and 1 lymphoma) and 8 (7 PTCs and 1 follicular carcinoma) respectively; 5 (62.5%) and 5 (62.5%) of them were correctly diagnosed by criteria set 3.

Discussion

Thyroid nodules detected by palpation or radiography method are recommended to be evaluated by US to assess possible malignancy [1]. Nevertheless, it is difficult for conventional US to distinguish malignant thyroid nodules without highly suspicious features on US from authentic benign nodules.

The mean size of malignant nodules was statistically smaller than that of benign nodules in accordance with previous studies [3, 10, 30]. With regard to the US features, there was statistically significant difference in background of Hashimoto's thyroiditis, which is consistent with previous studies that higher prevalence of thyroid cancer was found coexisting with Hashimoto's thyroiditis than in the overall population [31, 32]. Complete solid component and hypoechogenicity were more commonly found in malignant thyroid nodules in this series. However, their specificities were hampered since up to 55% of benign nodules were hypoechoic and 47.7-75.9% of benign nodules were solid [3, 4, 10]. Absence of halo sign was more frequently found in malignant thyroid nodules, which is in agreement with previous studies [9, 10, 33].

In the current study, the diagnostic performance of ARFI elastography for differentiation between malignant nodules without highly suspicious features on US and benign nodules was firstly evaluated. The sensitivity (80.0%) and specificity (89.7%) of ARFI-induced SE score in the current study were similar to those reported by Xu et al [10] and the cut-off point was also SE score-4. Thus, ARFI-induced SE could also be used for differential diagnosis in malignant thyroid nodules without highly suspicious features on US that would not cause any loss in diagnostic performance. For p-SWE, it had a higher sensitivity (80.0%) and lower specificity (57.9%) compared with several previous studies [9, 10, 21]. The mean SWV of benign nodules (2.02 m/s) was nearly the same as that in some previous studies (range: 2.10-2.34 m/s); while it was interesting that the mean SWV of malignant nodules without highly suspicious features on US (3.64 m/s) was markedly lower than that in previous studies (range: 4.82-6.34 m/s) [9, 10, 34]. As a consequence, the specificity of p-SWE decreased in comparison with general population. The finding indicates that the stiffness of thyroid malignant nodules without highly suspicious features on US is not as obvious as that of typical thyroid malignancies, which is possibly related to the uniform pathological changes in thyroid malignancy without highly suspicious features on US. However, future study is needed to confirm this hypothesis. Related to this, the cut-off point of SWV for p-SWE (2.15 m/s) was observably lower than that in the published reports (range: 2.42-2.87 m/s) [9, 10, 21, 25, 34, 35]. The result is relevant in clinical practice, which reminds us that a lower SWV value does not necessarily indicate a benign nodule. The thyroid malignancy without highly suspicious features on US should be excluded when making a diagnosis of benign nodule.

Distinguished from simple method of combination in previous studies [36, 37], 2 combination approaches were firstly evaluated in the current study. Criteria set 3 was either ARFI-induced SE or p-SWE, while criteria set 4 was the combination of ARFI-induced SE and p-SWE. Although no significant improvement were found for the combination criteria sets in terms of AUCs, the sensitivity reached the highest (92.5%) for criteria set 3 whereas the specificity was the highest (95.2%) for criteria set 4.

In addition, the accuracy was the highest (91.8%) for criteria set 4. Therefore, ARFI-induced SE or p-SWE should not be used independently. The two combination approaches should be considered together with an aim to achieve both high sensitivity and high specificity. As can be seen in the results section, the false positive and false negative nodules reduced significantly after applying the two combination approaches.

There were some limitations in the current study. Firstly, only nodules ≥5 mm were included because of the limit of 6×5 mm sampling ROI when measuring SWV of p-SWE. Therefore, malignant nodules of <5 mm might be omitted. However, thyroid malignancy <5 mm generally does not need aggressive management thus the limitation will not influence the clinical practice. Secondly, selection bias might be present for included patients who were referred for surgery, and it couldn't represent the situation of common population completely. Additionally, it was a single-center and retrospective study. Multi-center and prospective studies with large case series were needed to verify the usefulness of ARFI elastography in diagnosing thyroid malignancy without highly suspicious features on US.

Conclusions

ARFI elastography is helpful for differentiation between malignant thyroid nodules without highly suspicious features on US and real benign nodules. The combination of ARFI-induced SE and p-SWE leads to improved sensitivity and specificity. However, different combination methods should be applied. Finally, the stiffness in thyroid malignant nodules without highly suspicious features on US might be lower than that in typical thyroid malignancies; therefore, attention should be paid to make a benign diagnosis solely based on the results of SWV measurement on p-SWE.

Acknowledgements

This work was supported in part by Grant SHDC12014229 from Shanghai Hospital Development Center, Grant 14441900900 from Science and Technology Commission of Shanghai Municipality, Grant 2012045 from Shanghai Municipal Human Resources and Social Security Bureau, and Grant 81401417 from the National Natural Science Foundation of China.

Disclosure of conflict of interest

None.

Address correspondence to: Dr. Hui-Xiong Xu, Department of Medical Ultrasound, Shanghai Tenth People's Hospital, Ultrasound Research and Education Institute, Tongji University School of Medicine, No. 301 Yanchangzhong Road, Shanghai 200072, China. E-mail: xuhuixiong@126.com

References

[1] Cooper DS, Doherty GM, Haugen BR, Kloos RT, Lee SL, Mandel SJ, Mazzaferri EL, McIver B, Pacini F, Schlumberger M, Sherman SI, Steward DL, Tuttle RM. Revised American Thyroid Association management guidelines for patients with thyroid nodules and differentiated thyroid cancer. Thyroid 2009; 19: 1167-1214.

[2] Guth S, Theune U, Aberle J, Galach A, Bamberger CM. Very high prevalence of thyroid nodules detected by high frequency (13 MHz) ultrasound examination. Eur J Clin Invest 2009; 39: 699-706.

[3] Kwak JY, Han KH, Yoon JH, Moon HJ, Son EJ, Park SH, Jung HK, Choi JS, Kim BM, Kim EK. Thyroid imaging reporting and data system for US features of nodules: a step in establishing better stratification of cancer risk. Radiology 2011; 260: 892-899.

[4] Moon WJ, Jung SL, Lee JH, Na DG, Baek JH, Lee YH, Kim J, Kim HS, Byun JS, Lee DH. Benign and malignant thyroid nodules: US differentiation--multicenter retrospective study. Radiology 2008; 247: 762-770.

[5] Salmaslioğlu A, Erbil Y, Dural C, Işsever H, Kapran Y, Ozarmağan S, Tezelman S. Predictive value of sonographic features in preoperative evaluation of malignant thyroid nodules in a multinodular goiter. World J Surg 2008; 32: 1948-1954.

[6] Nam SY, Shin JH, Han BK, Ko EY, Ko ES, Hahn SY, Chung JH. Preoperative ultrasonographic features of papillary thyroid carcinoma predict biological behavior. J Clin Endocrinol Metab 2013; 98: 1476-14782.

[7] Kim EK, Park CS, Chung WY, Oh KK, Kim DI, Lee JT, Yoo HS. New sonographic criteria for recommending fine-needle aspiration biopsy of nonpalpable solid nodules of the thyroid. AJR Am J Roentgenol 2002; 178: 687-691.

[8] Frates MC, Benson CB, Charboneau JW, Cibas ES, Clark OH, Coleman BG, Cronan JJ, Doubilet PM, Evans DB, Goellner JR, Hay ID, Hertzberg

BS, Intenzo CM, Jeffrey RB, Langer JE, Larsen PR, Mandel SJ, Middleton WD, Reading CC, Sherman SI, Tessler FN. Management of thyroid nodules detected at US: Society of Radiologists in Ultrasound consensus conference statement. Radiology 2005; 237: 794-800.

[9] Zhang YF, Xu HX, He Y, Liu C, Guo LH, Liu LN, Xu JM. Virtual touch tissue quantification of acoustic radiation force impulse: a new ultrasound elastic imaging in the diagnosis of thyroid nodules. PLoS One 2012; 7: e49094.

[10] Xu JM, Xu XH, Xu HX, Zhang YF, Zhang J, Guo LH, Liu LN, Liu C, Zheng SG. Conventional US, US elasticity imaging, and acoustic radiation force impulse imaging for prediction of malignancy in thyroid nodules. Radiology 2014; 272: 577-586.

[11] Dustin SM, Jo VY, Hanley KZ, Stelow EB. High sensitivity and positive predictive value of fine-needle aspiration for uncommon thyroid malignancies. Diagn Cytopathol 2012; 40: 416-421.

[12] Renshaw AA. Sensitivity of fine-needle aspiration for papillary carcinoma of the thyroid correlates with tumor size. Diagn Cytopathol 2011; 39: 471-474.

[13] Berker D, Aydin Y, Ustun I, Gul K, Tutuncu Y, Işik S, Delibasi T, Guler S. The value of fine-needle aspiration biopsy in subcentimeter thyroid nodules. Thyroid 2008; 18: 603-608.

[14] Yoon JH, Lee HS, Kim EK, Moon HJ, Kwak JY. Thyroid Nodules: Nondiagnostic Cytologic Results according to Thyroid Imaging Reporting and Data System before and after Application of the Bethesda System. Radiology 2015; 276: 579-87.

[15] Kiernan CM, Broome JT, Solorzano CC. The Bethesda system for reporting thyroid cytopathology: a single-center experience over 5 years. Ann Surg Oncol 2014; 21: 3522-3527.

[16] Jo VY, Stelow EB, Dustin SM, Hanley KZ. Malignancy risk for fine-needle aspiration of thyroid lesions according to the Bethesda System for Reporting Thyroid Cytopathology. Am J Clin Pathol 2010; 134: 450-456.

[17] Tozaki M, Isobe S, Fukuma E. Preliminary study of ultrasonographic tissue quantification of the breast using the acoustic radiation force impulse (ARFI) technology. Eur J Radiol 2011; 80: e182-187.

[18] Yoneda M, Suzuki K, Kato S, Fujita K, Nozaki Y, Hosono K, Saito S, Nakajima A. Nonalcoholic fatty liver disease: US-based acoustic radiation force impulse elastography. Radiology 2010; 256: 640-647.

[19] Guo LH, Liu BJ, Xu HX, Liu C, Sun LP, Zhang YF, Xu JM, Wu J, Xu XH. Acoustic radiation force impulse elastography in differentiating renal solid masses: a preliminary experience. Int J Clin Exp Pathol 2014; 7: 7469-7476.

[20] Sporea I, Vlad M, Bota S, Sirli RL, Popescu A, Danila M, Sendroiu M, Zosin I. Thyroid stiffness assessment by acoustic radiation force impulse elastography (ARFI). Ultraschall Med 2011; 32: 281-285.

[21] Bojunga J, Dauth N, Berner C, Meyer G, Holzer K, Voelkl L, Herrmann E, Schroeter H, Zeuzem S, Friedrich-Rust M. Acoustic radiation force impulse imaging for differentiation of thyroid nodules. PLoS One 2012; 7: e42735.

[22] Zhang YF, Liu C, Xu HX, Xu JM, Zhang J, Guo LH, Zheng SG, Liu LN, Xu XH. Acoustic radiation force impulse imaging: a new tool for the diagnosis of papillary thyroid microcarcinoma. Biomed Res Int 2014; 2014: 416969.

[23] Friedrich-Rust M, Romenski O, Meyer G, Dauth N, Holzer K, Grünwald F, Kriener S, Herrmann E, Zeuzem S, Bojunga J. Acoustic Radiation Force Impulse-Imaging for the evaluation of the thyroid gland: a limited patient feasibility study. Ultrasonics 2012; 52: 69-74.

[24] Zhang YF, He Y, Xu HX, Xu XH, Liu C, Guo LH, Liu LN, Xu JM. Virtual touch tissue imaging on acoustic radiation force impulse elastography: a new technique for differential diagnosis between benign and malignant thyroid nodules. J Ultrasound Med 2014; 33: 585-595.

[25] Grazhdani H, Cantisani V, Lodise P, Di Rocco G, Proietto MC, Fioravanti E, Rubini A, Redler A. Prospective evaluation of acoustic radiation force impulse technology in the differentiation of thyroid nodules: accuracy and interobserver variability assessment. J Ultrasound 2014; 17: 13-20.

[26] Xu JM, Xu HX, Xu XH, Liu C, Zhang YF, Guo LH, Liu LN, Zhang J. Solid hypo-echoic thyroid nodules on ultrasound: the diagnostic value of acoustic radiation force impulse elastography. Ultrasound Med Biol 2014; 40: 2020-2030.

[27] Moon WJ, Baek JH, Jung SL, Kim DW, Kim EK, Kim JY, Kwak JY, Lee JH, Lee JH, Lee YH, Na DG, Park JS, Park SW. Ultrasonography and the ultrasound-based management of thyroid nodules: consensus statement and recommendations. Korean J Radiol 2011; 12: 1-14.

[28] Barr RG, Zhang Z. Effects of precompression on elasticity imaging of the breast: development of a clinically useful semiquantitative method of precompression assessment. J Ultrasound Med 2012; 31: 895-902.

[29] Hanley JA, McNeil BJ. A method of comparing the areas under receiver operating characteristic curves derived from the same cases. Radiology 1983; 148: 839-843.

[30] Moon HJ, Kwak JY, Kim MJ, Son EJ, Kim EK. Can vascularity at power Doppler US help predict thyroid malignancy. Radiology 2010; 255: 260-269.

[31] Konturek A, Barczynski M, Wierzchowski W, Stopa M, Nowak W. Coexistence of papillary

thyroid cancer with Hashimoto thyroiditis. Langenbecks Arch Surg 2013; 398: 389-394.
[32] Zhang L, Li H, Ji QH, Zhu YX, Wang ZY, Wang Y, Huang CP, Shen Q, Li DS, Wu Y. The clinical features of papillary thyroid cancer in Hashimoto's thyroiditis patients from an area with a high prevalence of Hashimoto's disease. BMC Cancer 2012; 12: 610.
[33] Horvath E, Majlis S, Rossi R, Franco C, Niedmann JP, Castro A, Dominguez M. An ultrasonogram reporting system for thyroid nodules stratifying cancer risk for clinical management. J Clin Endocrinol Metab 2009; 94: 1748-1751.
[34] Zhang FJ, Han RL. The value of acoustic radiation force impulse (ARFI) in the differential diagnosis of thyroid nodules. Eur J Radiol 2013; 82: e686-90.
[35] Hou XJ, Sun AX, Zhou XL, Ji Q, Wang HB, Wei H, Sun JW, Liu H. The application of Virtual Touch tissue quantification (VTQ) in diagnosis of thyroid lesions: a preliminary study. Eur J Radiol 2013; 82: 797-801.
[36] Trimboli P, Guglielmi R, Monti S, Misischi I, Graziano F, Nasrollah N, Amendola S, Morgante SN, Deiana MG, Valabrega S, Toscano V, Papini E. Ultrasound sensitivity for thyroid malignancy is increased by real-time elastography: a prospective multicenter study. J Clin Endocrinol Metab 2012; 97: 4524-4530.
[37] Sebag F, Vaillant-Lombard J, Berbis J, Griset V, Henry JF, Petit P, Oliver C. Shear wave elastography: a new ultrasound imaging mode for the differential diagnosis of benign and malignant thyroid nodules. J Clin Endocrinol Metab 2010; 95: 5281-5258.